Available online at www.sciencedirect.com
SCIENCE DIRECT
Journal of the European Ceramic Society 26 (2006) 1231–1236
www.elsevier.com/locate/jeurceramsoc

Nanoporous anatase ceramic membranes as fast-proton-conducting materials

M.T. Colomer *

Instituto de Cerámica y Vidrio, CSIC, C/ Kelsen no. 5, Campus de la Universidad Autónoma, 28049 Madrid, Spain

Received 22 July 2004; received in revised form 21 January 2005; accepted 23 January 2005
Available online 26 February 2005

Abstract

Nanoporous anatase ceramic membranes were prepared via particulate sol–gel processes. The calcined xerogels were mesoporous, with a BET surface area of 121 m^2/g, an average pore diameter of 5.8 nm and a pore volume of 0.236 cm^3/g. Proton conductivity of the membranes was measured as a function of temperature and relative humidity, R.H. When anatase membranes are treated at pH 1.5, the proton conductivity increased in the whole range of temperature and R.H. It indicates that the surface site density (number of water molecules per square nanometer) of these materials has a strong effect on conductivity. The proton conductivity of the studied anatase membranes followed an Arrhenius-like dependence on the temperature (from room temperature to 90 °C), in both treated and untreated membranes. A sigmoidal dependence of the conductivity on the R.H. was observed with the greatest increase noted between 58 and 81% R.H. in both treated and untreated anatase membranes. The highest value of proton conductivity was found to be 0.015 S/cm at 90 °C and 81% R.H., for treated anatase ceramic membranes. An increase of the conductivity could be achieved by means of longer times of treatment.

According to the activation energy values, proton migration in this kind of materials could be dominated by the Grotthuss mechanism in the whole range of R.H. The similar values of proton conductivity, lower cost and higher hydrophilicity of these membranes make them potential substitutes for perfluorosulfonic polymeric membranes in proton exchange membrane fuel cells (PEMFCs).

Keyword: Nanoporous anatase; Electrical conductivity; Fuel cells; TiO_2; Proton conduction

1. Introduction

At present, Nafion is one of the few materials that deliver the set of chemical and mechanical properties required to perform as a good electrolyte in proton exchange membrane fuel cells (PEMFCs).[1] However, Nafion membranes are very expensive, hard to synthesize and present environmental problems with regards to recycling and disposal of fluorinated polymers and their separation from the platinum catalysts used. They are susceptible to deformation on the basis of their repetition of absorption and desorption of water. Moreover, the detrimental problem for high temperature use of Nafion is the loss of grafted HSO_4 branches.[2] Over the last 10 years, the proton conductivity characteristics of porous glasses and xerogels have been the subject of growing interest due to their potential as solid electrolytes in sensors, fuel cells, etc.[3–8] In particular, both silica and acid doped silica xerogels have been widely studied.[4,7,8] However, other type of xerogels and porous ceramic membranes could also, in principle, display high values of proton conductivity.

Possible future electrolyte materials in PEMCs should provide high proton conductivity at low temperature; hydrophilicity and mechanical, thermal, and chemical stability. They should also be impermeable to H_2 and O_2. Stable inorganic membranes with high conductivities at low temperature, if developed, would extend usefulness beyond the limitation of both organic and hybrid films and would have potential viability.

High porosity and suitable pore size anatase ceramic membranes could be one of the most promising crystalline materials as electrolytes in PEMFCs. Anatase ceramic membranes

* Tel.: +91 735 58 58; fax: +91 735 58 43.
E-mail address: tcolomer@icv.csic.es.

0955-2219/$ – see front matter © 2005 Elsevier Ltd. All rights reserved.
doi:10.1016/j.jeurceramsoc.2005.01.035

are acid resistant and their precursor sols can produce coherent films. The use of these nanoporous membranes would require tube or flat technology fuel cell geometry to avoid contact between cathode and anode reagents. Furthermore, in order to fabricate oxide-based PEMFCs that are capable of keeping streams of H_2 and O_2 from mixing, a separation layer with an average pore size on the order of 1–4 nm whose pores are filled with water would be necessary.

TiO_2 particles loaded with Pt would be employed as the electrodes. The membrane electrode assemblies could be prepared by dip-coating or slip-casting techniques.

The sol–gel method is an excellent process for producing highly proton-conductive solid materials. The control of pore structure such as pore diameter and pore volume is very important for designing the proton conducting paths. Compared to polymeric sol–gel routes, sol–gel processing of particles offers a sharper pore-size distribution in the final product. In the first stage of this particulate sol–gel route, we should produce uniformly distributed particles in the nanometer-size range that match the pore scale required by the application. The second stage of this particulate sol–gel route is to transform the sol to a gel by evaporating the solvent.

The objective of this work is to design mesoporous anatase ceramic membranes of high porosity and small pore size (∼6.0 nm) by a particulate sol–gel route, with the aim of obtaining proton exchange electrolytes for PEMFCs. Electromotive force measurements were performed to determine the type of carrier responsible of the conduction process. A study of the electrical transport properties as a function of both temperature and relative humidity is reported. The effect of the surface site density on the electrical transport properties is also investigated.

2. Experimental

The TiO_2 sol was synthesized by the hydrolysis of titanium tetra-isopropoxide, $Ti(Opr^i)_4$ (98% Aldrich reagent grade and used as received). The titanium tetra-isopropoxide, was hydrolyzed in water into which concentrated nitric acid, HNO_3 (ACS), was previously added. Chemicals were purchased from Aldrich Chemical Inc., except for the nitric acid (70% ACS reagent grade), which was used as-received from Fischer. Dialysis tubing was employed to clean the sol after the hydrolysis and condensation reactions were complete (membrane tubing: Spectra/por, molecular cut-off = 3500 molecular weight). Precipitation occurred immediately upon hydrolysis. These precipitates were then peptized with the available HNO_3 at room temperature. The sols were put into dialysis tubing and dialyzed against pure water to remove nitric acid and isopropanol byproduct until the pH is 3.5.

In order to fabricate membranes with flat crack-free regions larger than 1 cm^2, the sols were dried in Teflon dishes at 25 °C and constant R.H. Titania sols were gelled rapidly (after 48 h) under low-R.H. conditions (30%) to minimize pore size in the dry xerogels, which were fired at 400 °C for 3 h in order to achieve the ceramic membranes. X-ray diffraction analysis of powdered xerogels was carried out with a D-5000 Siemens diffractometer using monochromatized Cu Kα radiation.

The average particle size in the prepared sols was determined by quasi-elastic laser light scattering using photon correlation spectroscopy on a Brookhaven light scattering instrument equipped with a laser light scattering goniometer (Model BI2030AT). The wavelength of the laser light used in this instrument was 633 nm, which can detect a minimal particle size of 3 nm. The porous structure of the ceramic membranes was characterized by nitrogen sorption (Micromeritics ASAP 2000 poresizer) after degassing. N_2 with molecule cross-sectional area of 0.162 nm^2 was used as the adsorptive gas. Prior to N_2 sorption, all samples were degassed [i.e. exposing the monoliths to a vacuum pressure lower than 1 Pa at 200 °C overnight (20 h)]. This is done to remove physically adsorbed gases from the sample surfaces, in particular water vapour.[9] The specific surface areas were estimated in relation to the masses of the outgassed samples. Three isotherms were collected for each sample to ensure that the data were representative. Pore size distributions were calculated from the desorption data using the BJH method.[10,11] Specific surface area was calculated from the BET equation. Pore volume was determined from the adsorption maxima. The connectivity of the membranes was calculated from the Seaton's model based on the use of the percolation theory.[12] The water contents of the ceramic membranes were measured by thermogravimetric analysis (TG/DTG) using a Netzsch STA 409 system. Samples were equilibrated at 81% R.H. before placing them in the balance crucible. Next, TG curves were registered under a dynamic dry air atmosphere of 20 mL/min and the following heating program: the temperature was increased to 350 °C at a rate of 1 °C/min. The membranes were exposed for several days to 81% R.H. to reach full surface hydroxylation/hydration before performing the TG analysis. For comparison, the same type of thermal analysis was performed on a strip of Nafion 117 film.

A hydrogen concentration cell similar to that reported by Nogami et al.[13] was constructed in order to determine the mobile species. For this, both surfaces of the ceramic membranes were covered with porous Ag paste and sealed by epoxy resin. Membranes of 1 cm diameter and 0.11 cm thickness were tested. The electromotive force generated between the electrodes was measured by a potentiostat (Model Voltalab 40) as a function of the hydrogen partial pressure. The total pressure of gases was constant at 1 atm and the gas flow rates were 150 mL/min. Both gases were moist and kept at a relative humidity of 81% at room temperature.

Electrical conductivity of the membranes was measured by electrochemical impedance spectroscopy (EIS) using a HP-4192A frequency response analyzer. The frequency range used was 5–10^7 Hz. Gold electrodes were sputtered onto both sides of each membrane prior to the electrical measurements. Before collecting impedance spectra, the calcined

membranes were allowed to equilibrate at different R.H. (33, 58, 75, 81 and 97%) for 24 h in sealed chambers containing saturated solutions of appropriate salts [$MgCl_2{\cdot}6H_2O$ for 33%, $NaBr{\cdot}2H_2O$ for 58%, NaCl for 75%, $(NH_4)_2SO_4$ for 81% and K_2SO_4 for 97% R.H.].[14] Measurements were performed at constant temperature (from 25 to 90 °C), with the sample chamber immersed in a thermostatically controlled water bath. The reproducibility of the results was verified by repeating the measurements three times for a given sample, and also by testing different samples of the same material equilibrated under the same conditions. The spectra were fit using the EQUIVCRT program by Boukamp.[15]

To study the effect of site density on electrical conductivity, the membranes were immersed at room temperature in a stirred HNO_3 solution at pH 1.5. The membranes were then rinsed with MQ water and left to dry at 120 °C overnight. We will refer to these samples as treated membranes.

3. Results and discussion

3.1. Nitrogen sorption

The N_2 adsorption–desorption isotherm for the anatase membranes is of type IV of the IUPAC classification, and exhibits a H1 hysteresis loop (Fig. 1).[16] The membranes were mesoporous, with a BET surface area of 121 m^2/g, an average pore diameter of 5.8 nm (desorption) (Fig. 2) and a pore volume of 0.236 cm^3/g. The calcined xerogels can be regarded as having high surface area and porosity (47.0%). The width of the hysteresis is indicative of the interconnectivity of these pores. The wider the hysteresis, the more interconnected are the pores. The value of the connectivity is 5.6 for the membranes according to the Seaton's model[12] indicating an open framework with an interconnected internal structure. Interconnection between pores is indispensable for achieving high proton conductivity.

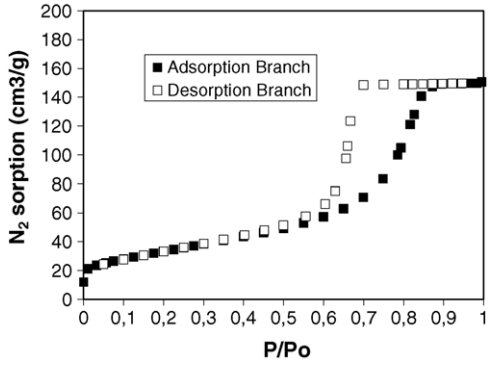

Fig. 1. Nitrogen adsorption–desorption isotherms of anatase membranes.

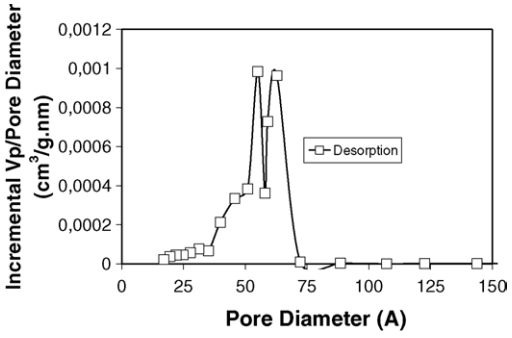

Fig. 2. Pore size distribution of anatase calcined xerogels.

3.2. XRD and DTA-TG measurements

The XRD patterns of the calcined xerogels at 400 °C for 3 h corresponds to anatase phase.

The ability of these xerogels and Nafion to retain water at different temperatures was studied by combined TGA and BET analysis.[17] Data extracted from this analysis are reported in Table 1.

As is well known, the adsorption energy for physisorbed water is smaller than for chemisorbed molecular water/hydroxyl groups.[18–20] Therefore, physisorbed and chemisorbed should be eliminated at different temperatures. The weight loss before 100 °C in the TG curves is assigned to physisorbed water, and the loss between 100 and 350 °C to surface hydroxyl groups and/or coordinated water.[17] Under the experimental conditions used in these measurements, the exposure of the membranes to a solution at pH 1.5 increases the total amount of water (physisorbed + chemisorbed) from 62.2 (untreated sample) to 73.9 molecules/nm^2 (treated membrane). Thus, protonation increases the water uptake of the membranes; this was observed over the full range of R.H.

Under the above-mentioned experimental conditions, the anatase membranes show a higher water content per unit volume (26 mmol/cm^3 for the untreated calcined xerogel and 30 mmol/cm^3 for the treated membrane, respectively) than that of Nafion (15 mmol/cm^3), which implies a higher hydrophilicity for the anatase membranes. The results show that oxides retain a larger amount of water in their pores, which is expected since their surfaces are more hydrophilic than Nafion. Furthermore, the temperatures found for the DTG minimum of the anatase membranes provides evidence that the thermal stability of the physisorbed water is 80 °C for the ceramic membranes and lower for Nafion (60 °C). Moreover, between 100 and 200 °C, the percentage of water remaining in the membranes is higher than in Nafion, which may enable these calcined xerogels to maintain relatively high proton conductivity at temperatures above 100 °C.

Table 1
Water content per volume of sample in samples hydrated at 25 °C and 81% R.H.

Material	Water content (mmol/cm^3)
TiO_2	26
TiO_2 (after protonation)	30
Nafion	15

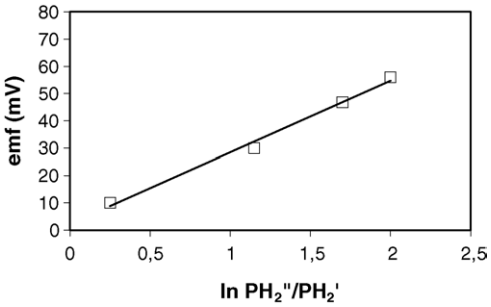

Fig. 3. Relationship between emf and the relative hydrogen gas pressure at room temperature and 81% R.H.

3.3. Electrical properties

3.3.1. EMF measurements

Before the impedance spectroscopy measurements were performed, EMF values at steady state as a function of the logarithm of hydrogen partial pressure were obtained. Those values satisfied a linear relationship between emf and $\ln p''H_2/p'H_2$ (Fig. 3). The constant number in the Nernstian equation is estimated as 1.8 ± 0.03, and is close to a theoretical value of 2, indicating that hydrogen reacts according to the reaction $H_2 = 2H^+ + 2e^-$, and the protons travel through the membrane. This interpretation is in agreement with Nogami et al.[13] who obtained an estimated value of 2.2 for porous sol–gel derived glasses of $P_2O_5{\cdot}SiO_2$.

3.3.2. Impedance spectroscopy

Fig. 4 shows the impedance spectra of the TiO_2 membranes at 25 °C for different R.H. values. The membrane resistance was considered to be the intersection of the arc with the Z (real) axis at lower frequencies as this value was independent of the different applied bias voltages, applied on top of the oscillating potential. At lower R.H. (33 and 58% R.H.), the impedance plot consisted of one semicircle in series with a spike (constant phase element, CPE) that can be associated to the membrane-electrode interface response. For higher R.H. (81 and 97% R.H.), two resistance values can be determined from the impedance spectra. One of the proton mobilities could be related to that of the protons travelling through the layer of clusters along the walls (higher resistance value) and the second one could be associated to the mobility of the protons in the bulk-like water filling the pores (lower resistance value), in accordance with the uptake of physisorbed water is a two-regime process.[20]

Fig. 5 shows the proton conductivity values for both untreated and treated anatase membranes at room temperature for different R.H. values. The dependence of the conductivity is sigmoidal mode for both cases and according to the classification of the proton conductors as a function of the water vapor partial pressure proposed by Colomban and Novak,[21] the titania calcined xerogels behave between an intrinsic conductor and a surface conductor. Data show (Fig. 5) that the conductivity improves with R.H. For the untreated membranes, the change in conductivity is small (from 2.59×10^{-6} to 8.38×10^{-6} S/cm) for lower relative humidities (from 33 to 58% R.H.) and exhibits a radical change at high R.H. values (from 8.38×10^{-6} S/cm at 58% R.H. to 1.26×10^{-3} S/cm at 81% R.H.). Thus, the proton conductivity increases almost 3 orders of magnitude when the relative humidity increases from 33 to 81% R.H. for the untreated ceramic membrane. For the treated membrane, the conductivity increases more than 1 order of magnitude when the R.H. increases from 33 to 81%. In both cases, the conductivity shows the highest increase between 58 and 81% R.H. This testifies that the uptake of adsorbed water is a two-regime process. This mechanism of water adsorption was proposed by Dubinnin and Serpinsky (D.S. theory).[20] At lower R.H., the water forms a layer of clusters along the walls of a matrix of interconnected pores. At higher R.H., new water molecules start filling the remaining pore space through capillary condensation.

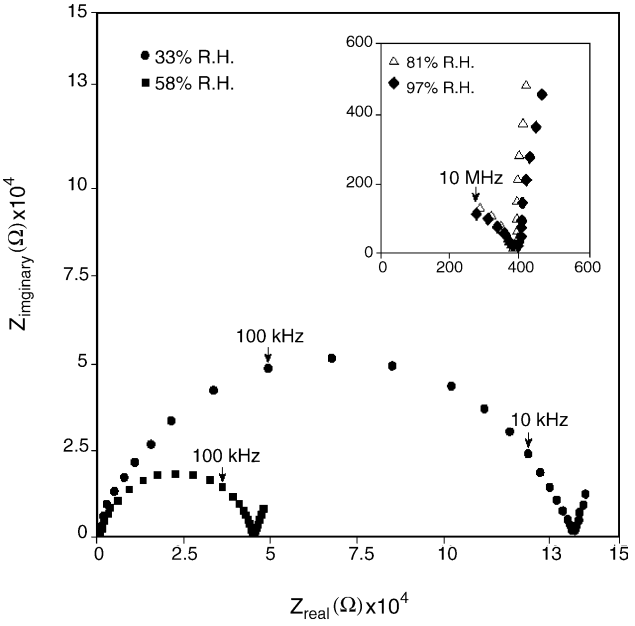

Fig. 4. Impedance spectra of an untreated ceramic membrane at different R.H. values.

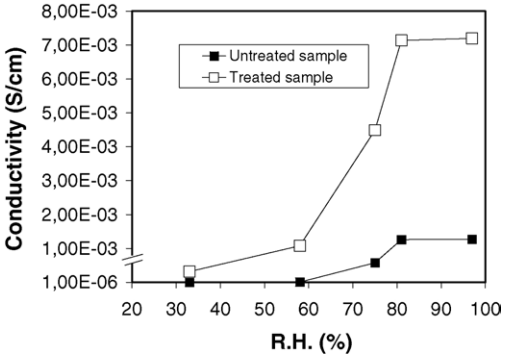

Fig. 5. Proton conductivity values at room temperature vs. different R.H. for both untreated and treated membranes.

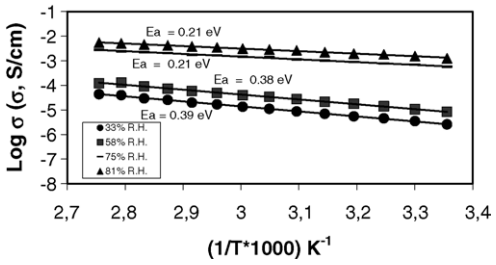

Fig. 6. Logarithm of the proton conductivity vs. the reciprocal of the temperature at different R.H. for an untreated membrane.

As the R.H. is controlled by using saturated salts, and the % R.H. for these salts depends on temperature, the conductivity for the system from 40 to 90 °C may correspond to lower values of R.H.

3.3.3. Arrhenius plots. Activation energy

Fig. 6 depicts the proton conductivity of the untreated TiO_2 ceramic membranes at different relative humidities versus the reciprocal of temperature (from 25 to 90 °C). An Arrhenius-like dependence on temperature is observed in all cases. At 90 °C and 81% R.H., the proton conductivity is 5.50×10^{-3} S/cm. The values of the activation energy (E_a) were obtained by linear regression of the Arrhenius equation $\sigma = \sigma_0 \exp(-E_a/kT)$, where σ_0 is a pre-exponential parameter and k is the Boltzmann's constant. The activation energy values for each relative humidity are registered in Fig. 6. According to those values, proton migration is dominated by the Grotthuss mechanism. In this mechanism, the proton forms a H_3O^+ ion and jumps to the neighboring lone pair of electrons of a water molecule. For such a mechanism, the activation energy for proton conduction should be about 0.14–0.40 eV.[21] The decrease in the activation energies when relative humidity increases can be explained from the higher water content. The filling up of channels by water molecules leads to higher conductivity, not only via the σ_0 factor, which is proportional to the number of mobile species, but also by increasing the dynamical disorder.[22]

Fig. 7 depicts the proton conductivity of the treated TiO_2 membranes at different relative humidities versus the reciprocal of temperature (from 25 to 90 °C). An Arrhenius-like dependence on temperature is also observed for every R.H. At 90 °C and 81% RH, the proton conductivity for the treated membranes is 0.015 S/cm, 1 order of magnitude higher than the untreated membrane and in the same order of Nafion for the same conditions.[23,24] A further study with longer treatment times with HNO_3 acid is necessary to achieve membranes with higher conductivity values.

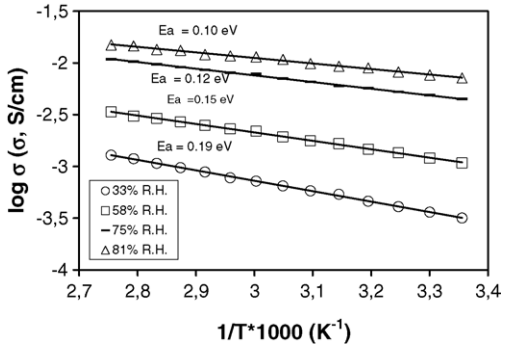

Fig. 7. Logarithm of the proton conductivity vs. the reciprocal of the temperature at different R.H. for a treated calcined xerogel.

Activation energies are larger for the untreated membranes than for the treated ones. This result can be explained on the basis of a higher site density to which the water can adsorb for the treated sample: As a consequence, the distance between water molecules will be lower and the proton hopping along the channels will be easier. On the other hand, water structure is changed by the presence of the pore walls. The degree of perturbation is related to the magnitude and distribution of the interfacial charge.[25] It is known that the structure of water in a cluster influences the activation energy of proton hopping.[25] The treated materials will have a different water structure since they have a more positive surface charge than the untreated membranes, and this could affect the mobility of the proton. In summary, according to the activation energy values found, proton migration is dominated by the Grotthuss mechanism in the whole range of R.H. in both the untreated and the treated materials.

The similar values of proton conductivity, lower cost and higher hydrophilicity of nanoporous anatase membranes make them potential substitutes for Nafion membranes in proton exchange membranes fuel cells (PEMFCs).

4. Conclusions

Nanoporous anatase membranes were prepared via particulate sol–gel processes. According to EMF measurements, electrical transport is due to protons in this kind of material. Proton conductivity showed a pronounced dependence with R.H., on the greatest increase observed between 58 and 81% R.H. The proton conductivity of the studied membranes followed an Arrhenius-like dependence on the temperature. The highest value of proton conductivity was found to be 0.015 S/cm at 90 °C and 81% R.H., for HNO_3 acid treated membranes. An increase of the surface site density of the calcined xerogels enhances their electrical conductivity. According to the activation energy values, proton migration is dominated by the Grotthuss mechanism in the whole range of R.H. in both the untreated and treated membranes.

Acknowledgments

This work is in the frame of the contracts CAM 07N/0102/2002 and CICYT MAT2002-00250.

References

1. Kreuer, K. D., On the development of proton conducting materials for technological applications. *Solid State Ionics*, 1997, **97**, 1–15.
2. Gruger, A., Régis, A., Schmatko, T. and Colomban, Ph., Nanostructure of nafion membranes at different states of hydration: an IR and Raman study. *Vib. Spectrosc.*, 2001, **26**, 215–225.
3. Nogami, M., Nagao, R. and Wong, C., Proton conduction in porous silica glasses with high water content. *J. Phys. Chem. B*, 1998, **102**, 5772–5775.
4. Colomer, M. T. and Anderson, M. A., High porosity silica xerogels prepared by a particulate sol–gel route: pore structure and proton conductivity. *J. Non-Cryst. Solids*, 2001, **290**, 93–104.
5. Matsuda, A., Kanzaki, T., Tadanaga, K., Tatsumisago, M. and Minami, T., Medium temperature range characterization as a proton conductor for phosphosilicate dry gels containing large amounts of phosphorus. *Electrochim. Acta*, 2001, **47**, 939–944.
6. Anappara, A. A., Rajeshkumar, S., Mukundan, P., Warrier, P. R. S., Ghosh, S. and Warrier, K. G. K., Impedance spectroscopic studies of sol–gel derived subcritically dried silica aerogels. *Acta Mater.*, 2004, **52**, 369–375.
7. Mioc, U. B., Milonjic, S. K., Stamenkovic, V., Radojevic, M., Colomban, Ph., Mitrovic, M. M. *et al.*, Structural properties and proton conductivity of the 12-tungstophosporic acid doped aluminosilicate gels. *Solid State Ionics*, 1999, **125**, 417–424.
8. Mioc, U. B., Milonjic, S. K., Malovic, D., Stamenkovic, V., Colomban, Ph., Mitrovic, M. M. *et al.*, Structure and proton conductivity of 12-tungstophosporic acid doped silica. *Solid State Ionics*, 1997, **97**, 239–246.
9. Lowell, S. and Shields, J. E., *Powder Surface Area and Porosity*. Chapman and Hall, London, New York, 1991.
10. Sing, K. S. W., Everett, D. H., Haul, R. A. W., Moscou, L., Pierotti, R. A., Rouquerol, J. *et al.*, Reporting physisorption data for gas solid systems with special reference to the determination of surface-area and porosity (recommendations 1984). *Pure Appl. Chem.*, 1985, **57**, 603–619.
11. Barret, E. P., Joyney, L. G. and Halenda, P. P., The determination of pore volume and area distributions in porous substances. I. Computations from nitrogen isotherms. *J. Am. Chem. Soc.*, 1951, **73**, 373–380.
12. Seaton, N. A., Determination of the connectivity of porous solids from nitrogen sorption measurements. *Chem. Eng. Sci.*, 1991, **46**, 1895–1909.
13. Nogami, M., Matsushita, H., Kasuga, T. and Hayakawa, T., Hydrogen gas sensing by sol–gel-derived proton-conducting glass membranes. *Electrochem. Solid State Lett.*, 1999, **2**, 415–417.
14. Lide, D. R., editor-in-chief, *Handbook of Chemistry and Physics* (*84th ed.*). CRC Press, 2003–2004.
15. Boukamp, B., *Equivalent circuit (EQUIVCRT. PAS)*. University of Twente, Twente, The Netherlands, 1988–1989.
16. Gregg, S. J. and Sing, K. S. W., *Adsorption, surface area and porosity*. Academic Press, London, 1982.
17. Vendange, V. and Colomban, Ph., Determination of the hydroxyl content in gels and porous "glasses" from alkoxide hydrolysis by combined TGA and BET analysis. *J. Porous Mater.*, 1996, **3**, 193–200.
18. Salame, I. I., Baagrev, A. and Bandosz, T. J., Revisiting the effect of surface chemistry on adsorption of water on activated carbons. *J. Phys. Chem. B*, 1999, **103**, 3877–3884.
19. McCallum, C.-L., Bandosz, T. J., McGrother, S. C., Müller, E. A. and Gubbins, K. E., *Langmuir*, 1996, **15**, 533–544.
20. Dubinin, M. M. and Serpinsky, V. V., Isotherm equation for water-vapor adsorption by microporous carbonaceous adsorbents. *Carbon*, 1981, **19**, 402–403.
21. Colomban, P. and Novak, A., In *Proton Conductors*, ed. P. Colomban. Cambridge University, Cambridge, Great Britain, 1992, pp. 38–55.
22. Kreuer, K. D., Stoll, I. and Rabenau, A., Proton conductivity of $H_3OUO_2AsO_4{\cdot}3H_2O$ (HUAs) under pressure indication for transition from vehicle mechanism to Grotthuss mechanism. *Solid State Ionics*, 1983, **9–10**, 1061–1064.
23. Gottesfeld, S. and Zawodsinski, T. A., In *Polymer Electrolyte Fuel Cells. Advances in Electrochemical Science and Engineering*, ed. R. C. Alkire, H. Gerischer, D. M. Kolb and C. W. Tobias. Wiley–VCH, Weinheim, 1997, pp. 245–263 (Chapter 5).
24. Marrink, S. J., Berkowitz, M. and Berendsen, H. J. C., Molecular-dynamics simulation of a membrane water interface—the ordering of water and its relation to the hydration force. *Langmuir*, 1993, **9**, 3122–3131.
25. Agmon, N., Hydrogen bonds, water rotation and proton mobility. *J. Chim. Phys. Phys.-Chim. Biol.*, 1996, **93**, 1714–1736.